Identification of Two Heme-Binding Sites in the Cytoplasmic Heme-Trafficking Protein PhuS from *Pseudomonas aeruginosa* and Their Relevance to Function[†]

Darci R. Block,[‡] Gudrun S. Lukat-Rodgers,[‡] Kenton R. Rodgers,*[,‡] Angela Wilks,[§] Mehul N. Bhakta,[§] and Ila B. Lansky[§]

Department of Chemistry, Biochemistry and Molecular Biology, North Dakota State University, 1231 Albrecht Avenue, Fargo, North Dakota 58105, and Department of Pharmaceutical Sciences, School of Pharmacy, 20 Penn Street, University of Maryland, Baltimore, Maryland 21201

Received July 28, 2007; Revised Manuscript Received September 25, 2007

ABSTRACT: PhuS is a cytoplasmic, 39 kDa heme-binding protein from *Pseudomonas aeruginosa*. It has previously been shown to transfer heme to its cognate heme oxygenase. It is expressed from the *phu* operon, which encodes a group of proteins known to actively internalize and transport heme from host organisms. This study combines the spectral resolution of resonance Raman spectroscopy with site-directed mutagenesis to identify and characterize the heme-bound states of holo-PhuS. This combined approach has identified a site in monomeric PhuS having alternate His ligands at positions 209 and 212. A second distinct binding site is present in dimeric PhuS. This site supports six-coordinate, low-spin heme, even when both His209 and His212 are mutated to Ala. The presence of conserved His and Tyr residues in all of the homologs characterized to date suggest that the dimer could be of the domain-swapped type in which two protein molecules are cross-linked by bound heme. The multiple heme-bound states and their sensitivity to pH suggest the possibility that these cytoplasmic heme-binding proteins have multiple functions that are toggled by variations in intracellular conditions.

Establishment of infection by bacterial pathogens relies on a readily available iron source. A considerable body of work in the area of bacterial genetics points to heme from host proteins as that source (*1*, *2*). A major source of iron is the host's hemoglobin and other heme proteins (*1*). Proteins involved in the uptake and intracellular transport of heme have been referred to in the literature as heme-binding proteins, heme transport proteins, heme-trafficking proteins, heme chaperones, and hemophores (*3*). The heme uptake and transport stages of bacterial iron assimilation systems in Gram-negative bacteria have a number of components in common, including proteins that function at the cell surface, in the periplasm, on the inner membrane, and in the cytosol. On the outer membrane, a TonB-dependent receptor uses proton motive force for active internalization of heme. A periplasmic binding protein shuttles the heme across the periplasm and transfers it to an ATP binding cassette for active transport across the inner membrane. Finally, in the case of the Gram-negative organism *Pseudomonas aeruginosa*, the cytoplasmic-trafficking protein PhuS delivers heme to a heme-degrading heme oxygenase (HO)[1] enzyme.

PhuS is a 39 kDa cytoplasmic protein encoded on the *phu* operon (*4*). The proposed function of PhuS is delivery of heme to the heme oxygenase *Pa*HO, which degrades the protoporphyrin-IX ligand, thereby producing biliverdin along with a molecule of CO and releasing iron (*5*). The transfer of heme between PhuS and *Pa*HO has been shown to be specific and is preceded by formation of a holo-PhuS−apo-*Pa*HO complex. In addition to PhuS, several other cytoplasmic heme-trafficking homologs have been investigated; HemS from *Yersinia enterocolitica* (*6*), ChuS from *Escherichia coli* (*7*, *8*), and ShuS from *Shigella dysenteriae* (*9*, *10*). PhuS, ShuS, and HemS have been proposed to deliver heme to the appropriate HO for degradation. $ChuS_{His6N}$ has been reported to exhibit HO activity (*7*), despite its lack of structural similarity with any known HO. However, whether the reported heme degradation reaction proceeds with regiospecific porphyrin ring opening and a turnover number greater than one has yet to be addressed. Heme oxygenase activity of ChuS notwithstanding, it carries 66% sequence identity and striking structural similarity to HemS (*6*). In contrast to ChuS, HO activity has not been reported for HemS, PhuS, or ShuS. On the basis of the crystal structures of apo- and holo-HemS from *Y. enterocolitica*, a "heme-induced fit" model for heme binding, wherein heme enters the binding pocket of an open conformer and induces conformational changes to yield a closed, heme-bound form, was proposed (*6*). Both HemS and ChuS structures reveal conformational reorganization of the secondary structure elements, especially the helices, of the C-terminal domain upon heme binding. The His residues 193 and 196, which occur in the C-terminal domains of ChuS and HemS,

[†] This work was supported by NIAID 1R15AI072719-01 (K.R.R.), NCRR P20RR15556 (K.R.R.), and National Institutes of Health Grant AI-48551 (A.W.).

* To whom correspondence should be addressed. Phone: (701) 231-8746. Fax: (701) 231-8831. E-mail: kent.rodgers@ndsu.edu.

[‡] North Dakota State University.

[§] University of Maryland.

[1] Abbreviations: 5c, five-coordinate; 6c, six-coordinate; HO, heme oxygenase; HS, high spin; LS, low spin; *Pa*HO, heme oxygenase from *P. aeruginosa*; rR, resonance Raman.

10.1021/bi701509n CCC: $37.00
Published on Web 11/20/2007

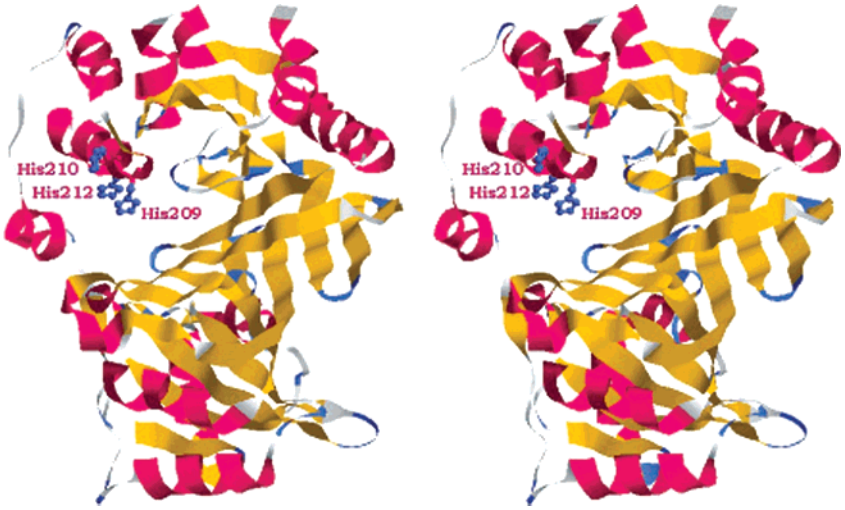

FIGURE 1: Cross-eyed stereo view of the homology-based structure model of apo-PhuS. The model is based on the crystal structure of apo-ChuS. The blue ball-and-stick side chains show the positions of His209, His210, and His212.

respectively, are axial heme ligands (*6*−*8*). They are homologous to His209 in PhuS.

This report presents additional biochemical and spectroscopic characterization of PhuS, which was carried out to further clarify the structural and dynamic properties of the immediate heme environment. Alignments of the cytoplasmic heme-binding proteins indicate sequence identities ranging from 39% to 98%. Similar comparisons have been made between sequences of siderophore and cobalamin transporters where, despite the striking similarities in their crystal structures, sequence homologies are only 20−30% (*11*). With the anticipation of structural similarity between PhuS and its homologs, HemS (*6*) and ChuS (*7*, *8*), the structure of PhuS has been modeled based on the apo-ChuS structure using SwissModel (*12*−*14*). The resulting structure, which is shown in Figure 1, provided the basis for the mutagenesis strategy used here to dissect the heme coordination chemistry of holo-PhuS. There are three histidine residues on the predicted heme-binding helix. They are His209, a conserved histidine, and His210 and His212, neither of which is conserved. These three residues were targeted for mutation with the goal of identifying the heme carrier ligand in PhuS and to clarify the basis for heme heterogeneity that was reported previously for holo-PhuS (*5*). These mutants and their CO complexes were investigated using UV−vis absorbance and resonance Raman (rR) spectroscopies to probe the axial bonding and peripheral nonbonding interactions between the heme and the heme pocket in PhuS. Those results are presented herein and reveal His209 as a proximal ligand in wild-type holo-PhuS. Moreover, in the absence of His209, the protein provides another histidine ligand, His212. When both of these histidines are mutated, the protein binds heme as a distinct 5c hydroxide complex. It is clear that replacement of the histidine carrier ligand with the noncoordinating amino acid, alanine, does not preclude heme binding. This demonstrates conformational flexibility of the protein and coordinative versatility that are manifested in stabilization of distinct heme-bound states. The accessibility of multiple holo-PhuS states having distinct protein-based axial ligands is the first evidence among this class of cytoplasmic heme-binding proteins that mechanisms of heme binding and/or release could involve one or more intramolecular axial ligand exchange steps.

EXPERIMENTAL PROCEDURES

Mutagenesis was carried out utilizing the polymerase chain reaction based Quickchange mutagenesis kit (Stratagene, La Jolla, CA). Oligonucleotides were designed to have melting temperatures (T_m) between 65 and 75 °C. The respective histidine mutants were verified by DNA sequencing of the gene constructs (Biopolymer Laboratory, University of Maryland, School of Medicine, University of Maryland). Expression, isolation, and chromatographic purification of PhuS(WT) and the reported histidine mutants were carried out as previously described (*5*). Separation of monomeric, dimeric, and trimeric forms of PhuS was accomplished by FPLC using a 1 cm × 40 cm Superdex 200 column.

Resonance Raman Spectroscopy. Resonance Raman scattering was excited using 413.1 and 441.6 nm emission from Kr^+ and HeCd lasers, respectively. Raman-scattered light was collected with *f*1 optics in the 135° back-scattering geometry, passed through a holographic notch filter, and *f* matched to a *f*4.5 0.6 m spectrograph fitted with a LN_2-cooled CCD detector. The entrance slit was set to 0.8 cm^{-1} for all measurements. The laser beam was focused to a line on the sample, and its power was adjusted to 2−4 mW for 413.1 nm excitation of the CO samples and 20 mW for Fe(II) samples. The power of the 441.6 nm laser beam was 7 mW. Spectra were recorded at ambient temperature, and all samples were spun at ∼20 Hz to minimize laser-induced degradation of the protein samples. The spectral windows were calibrated using Raman bands from methylene bromide, toluene, DMF, acetone, and ^{2}H-DMSO.

PhuS Sample Preparation. Ferrous PhuS(WT) and mutants samples were prepared by equilibration of the ferric protein solutions under a purge of water-saturated N_2 followed by reduction with a 10-fold excess of buffered sodium dithionite solution. The corresponding CO adducts were prepared anaerobically on a Schlenk line by equilibrating the protein solution under 1 atm of either CO or ^{13}CO and adding an excess of buffered sodium dithionite solution at pH 8.0.

Samples for spectrophotometric pH titrations were prepared by analytical dilution of protein stock solutions into

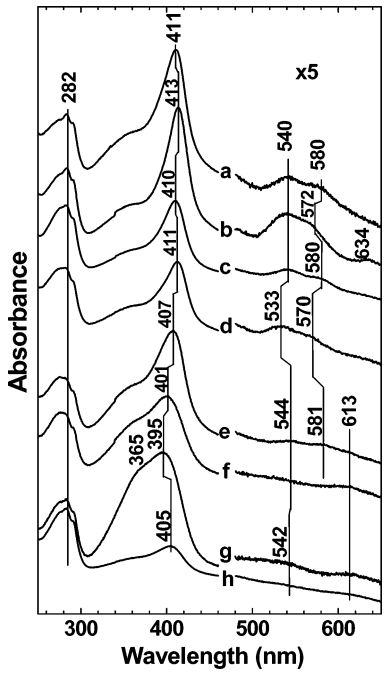

FIGURE 2: UV−vis absorbance spectra of (a) monomeric PhuS-(WT), (b) dimeric WT, (c) H210A (58%), (d) H209A (28%), (e) H212A (98%), (f) H209Y (97%), (g) H209A/H212A (90%), (h) H209A/H210A (73%) in 20 mM Tris−HCl, pH 8.0. Numbers in parentheses indicate percentage monomer.

20 mM MES, HEPES, and CHES adjusted to pHs ranging from 6.0 to 10.5. The pK_a's were calculated from a series of UV−vis absorbance spectra recorded from pH 5.5 to 12 using a commercial global analysis software package. The rR samples were similarly prepared in 5 mm NMR tubes.

RESULTS

Heme Environment in Ferric PhuS

Site-directed mutagenesis was used to analyze the effects of specific histidine variants on the bound heme of holo-PhuS. The following PhuS histidine mutants were generated: conserved His209 to Ala and Tyr, nonconserved His210 to Ala and His212 to Ala, and the double-histidine mutants (H209A/H210A) and (H209A/H212A). The following spectroscopic data are presented to address the identity of the axial heme ligand(s) and to characterize the conformational flexibility thought to play a role in the mechanism by which these proteins bind and release heme.

Ferric UV−Vis and rR Spectra at pH 8. The UV−vis spectra of the ferric PhuS proteins at pH 8.0 are shown in Figure 2. The top section of Table 1 lists the wavelengths of maximum absorbance for the ferric state of PhuS(WT) and the histidine mutants reported here. Their Soret maxima fall near 410 nm, except for (H209Y) and (H209A/H212A), which occur at 401 and 395 nm, respectively. The ratio of Soret absorbance to that at 280 nm indicates the extent to which the protein has been loaded with heme. PhuS(H209A/H210A) was isolated with the lowest A_{410}/A_{280} ratio of the mutants reported here, suggesting that it is not fully heme loaded. The rR spectra that correspond to these visible spectra are shown in the low-frequency (Figure 3A) and high-frequency (Figure 3B) regions. Monomeric holo-PhuS(WT) (Figure 3Aa) comprises a mixture of 5cHS and 6cLS heme, whereas the dimer (Figure 3Bb) is predominantly 6cLS. The shapes of the UV−vis spectra in Figure 2 are consistent with the rR features. The mixture of spin states and the identity of the axial ligand in monomeric PhuS(WT) can be explained by comparing the rR spectra of PhuS(H209A) (Figure 3Bd), (H212A) (Figure 3Be), (H209A/H210A) (Figure 3Bf), and (H209A/H212A) (Figure 3Bg) at pH 8.0. This region of the spectrum contains bands corresponding to in-plane porphyrin modes whose frequencies, by virtue of their sensitivities to metal ion radius (or porphyrin core size), are characteristic of iron spin state, oxidation number, and coordination number (*15*−*18*). The largest deviation in rR signature from that of PhuS(WT) in Figure 3B is an increase in 5cHS heme upon mutation of the axial histidine(s). The amount of 5cHS heme, indicated by the relative intensity of υ_3 at 1488 cm^{-1}, increases in the order (H209A), (H212A), (H209A/H210A), (H209A/H212A), (H209Y), from top to bottom of Figure 3B. The frequency and large intensity of υ_3 compared to υ_4 of (H209Y) and (H209A/H212A) indicate the axial ligand is likely anionic and coordinates through an oxygen atom. Thus, the axial ligands in (H209A/H212A) and (H209Y) are proposed to be hydroxide and tyrosinate, respectively.

Spectrophotometric pH Titrations of Ferric PhuS(WT), (H209A), (H210A), and(H212A). The pH-dependent behavior of the histidine mutants, PhuS(H209A), (H210A), and (H212A) as they compare to (WT), supports assignment of the axial histidine ligand. Analysis of the spectrophotometric titrations yielded pK_a's for their acid/base transitions. Figure 4A shows pH titration curves of PhuS(H209A), (H210A), and (H212A) overlaid on PhuS(WT). The PhuS(H210A) and (H212A) data were fit to a two-pK_a model with pK_{a1} = 7.1 ± 0.1 and pK_{a2} = 10.6 ± 0.2 for (H210A) and pK_{a1} = 7.4 ± 0.1 and pK_{a2} = 11.5 ± 0.1 for (H212A), similar to the values reported for PhuS(WT) (7.2 ± 0.1 and 10.2 ± 0.5) (*5*). In contrast, the PhuS(H209A) data were fit to a single-pK_a model with pK_{a1} = 8.9 ± 0.1. Figure 4B shows the corresponding speciation diagrams calculated from these pK_a values. These data clearly show that mutation of His209 elicits distinct acid−base behavior of the heme in holo-PhuS.

Resonance Raman Spectra of Ferric PhuS(WT) and His Mutants. Previous results from this laboratory showed that PhuS(WT) exists as a pH-dependent mixture of 6cLS, 6cHS, and 5cHS heme species with the 6cLS heme being favored in alkaline solution and HS heme favored at lower pH (*5*). In the present study, rR spectra of PhuS(H209A), (H210A), (H209A/H210A), (H212A), (H209Y), and (H209A/H212A) were all recorded over the pH range from 5 to 11.5. These spectra are shown in Figure 5.

The histidine mutants can be parsed into five categories (I−V) based on the pH dependence of their ferric rR spectra. The pH-dependent interconversions among heme species are revealed in these spectra by the interchange of intensity between the HS (green labels) and LS (red labels) marker bands in the panels of Figure 5. Table 2 lists the spin states and the identities of the axial ligands based upon (a) the data in Figures 5 and 7 and (b) the reasoning put forth in the following paragraphs.

Category I comprises PhuS(WT) and (H210A), which both have the conserved His209 and His212. The homology-based structure model (Figure 1) shows that the imidazole (ImH) side chains of these residues occur on the same face of the putative heme-binding helix. The rR spectra in Figure 5I

Table 1: Absorbance Maxima of Fe(III), Fe(II), and Fe(II)−CO PhuS (WT) and the Reported Histidine Mutants at pH 8

protein	species	Soret λ_{max} (nm)	Q bands λ_{max} (nm)	ref
PhuS(WT) mix	Fe(III)	410	545, 570	*5*
PhuS(WT) monomer		411	540, 580	this work
PhuS(WT) dimer		413.5	540, 566, 636 (CT)	this work
PhuS(H210A)		412	540, 578	this work
PhuS(H209A)		410	532, 566	this work
PhuS(H209Y)		400	530(sh), 608	this work
PhuS(H209A/H210A)		403	530, 614 (CT)	this work
PhuS(H212A)		407	544, 580	this work
PhuS(H209A/H212A)		395, 368 (sh)	537, 615	this work
hemin		394	572, 611 (CT)	this work
HO(H25A)		399	620	*26*
PhuS(WT)	Fe(II)	428	535, 559, 583 (sh)	*5*
PhuS(H210A)		430	526, 556, 587	this work
PhuS(H209A)		425	530, 560, 587 (sh)	this work
PhuS(H209Y)		425	532 (sh), 559, 588 (sh)	this work
PhuS(H209A/H210A)		430	522 (sh), 558, 592 (sh)	this work
PhuS(H212A)		418, 435 (sh)	533, 556, 576 (sh)	this work
PhuS(H209A/H212A)		420	559, 587	this work
HO(H25A)		426	551, 587	*26*
PhuS(WT)	Fe(II)−CO	420	541, 568	*5*
PhuS(H210A)		419	536, 569	this work
PhuS(H209A)		420	536, 569	this work
PhuS(H209Y)		418	533, 570	this work
PhuS(H209A/H210A)		417	536, 569	this work
PhuS(H212A)		417	536, 566	this work
PhuS(H209A/H212A)		409	534, 562	this work
hemin		408	533, 566	this work
HO(H25A) HO-1		411	533, 566	*26*
HO(H20A) HmuO		412	538, 568	*25*

show that the hemes in these proteins exist as pH-dependent mixtures of 5cHS, 6cHS, and 6cLS heme in which HS and LS hemes are favored at low and high pH, respectively. The 6cHS species at low pH is attributed to a complex with His and H_2O axial ligands, which is converted to a His/OH− complex in a HS−LS equilibrium at high pH (*5*). The spectral similarity of these two proteins and their similar pH behavior are consistent with two conclusions; (1) the axial ligands in these two proteins are the same, consistent with His209 and/or His212 coordination, and (2) His210 does not play a defining role in the heme coordination chemistry of holo-PhuS.

These conclusions were tested by mutating both His209 and His 212, leaving only His210 on the putative heme-binding helix. Figure 5II shows that without His209 and His212, the heme is essentially all 5c and HS. This is category II of the PhuS heme environments observed in this study. The increase in the intensity ratio $I(\upsilon_3)/I(\upsilon_4)$ (υ_4 is not shown) with increasing pH is consistent with the presence of a 5cHS heme with an O-bound anionic ligand (*19*). As PhuS contains only two tyrosine residues, which the homology model suggests are remote from the heme-binding helix, the alkaline form of PhuS(H209A/H212A) is most likely a 5cHS hydroxide complex. This raises the question of whether the heme is actually associated with the protein. This question was addressed by subjecting the protein to gel filtration chromatography and ultrafiltration with a MW cutoff of 30 kDa. Interestingly, the heme color remained with the protein in all cases. Taken together, these observations suggest that the nonbonded interactions between the heme and the protein provide sufficient driving force to form a stable heme complex. The rR spectra in Figure 5II further suggest that either His209, or His212, or both provide an endogenous ImH ligand to the heme in holo-PhuS. This conclusion is further supported by the rR spectrum of ferrous PhuS(H209A/H212A), which shows no evidence of a Fe−His stretching band, consistent with the absence of a Fe−His bond (vide infra). In contrast to the spectra in Figure 5II, a significant fraction of dimeric PhuS(H209A/H212A) is 6c and LS, as seen from the rR and UV−vis spectra in Figure 6. The presence of LS heme in the dimer of this mutant strongly suggests that a LS heme-binding site is created as a result of dimerization. This is consistent with a structure in which the two axial heme ligands are provided by different PhuS molecules (vide infra). The UV−vis spectrum of monomeric PhuS(H209A/H212A) (Figure 6, inset) is unique among the spectra of the mutants shown in Figure 2. Specifically, it exhibits a split Soret band typical of cofacial hemes. Such a cofacial arrangement would require association of two holo-PhuS(H209A/H212A) molecules, a conclusion that seems contrary to its having been separated from the dimer chromatographically. This behavior suggests that, in the absence of conformational constraints imposed by endogenous heme ligands, the flexibility of holo-PhuS accommodates loose association of the proteins. Similar behavior has been observed in the heme-binding protein ChaN (*20*). This loose complex likely dissociates on the gel filtration column, allowing it to be separated from the dimer. Its HS signature in the rR spectrum is consistent with pentacoordinate cofacial hemes, as has been observed for β-hematin and the malaria pigment (*21*). The ability to stabilize a heme-bound state without an $Fe-L_{axial}$ bond through loose association with another PhuS molecule leads to the interesting notion that such a state may be intermediate along a heme binding or release coordinate.

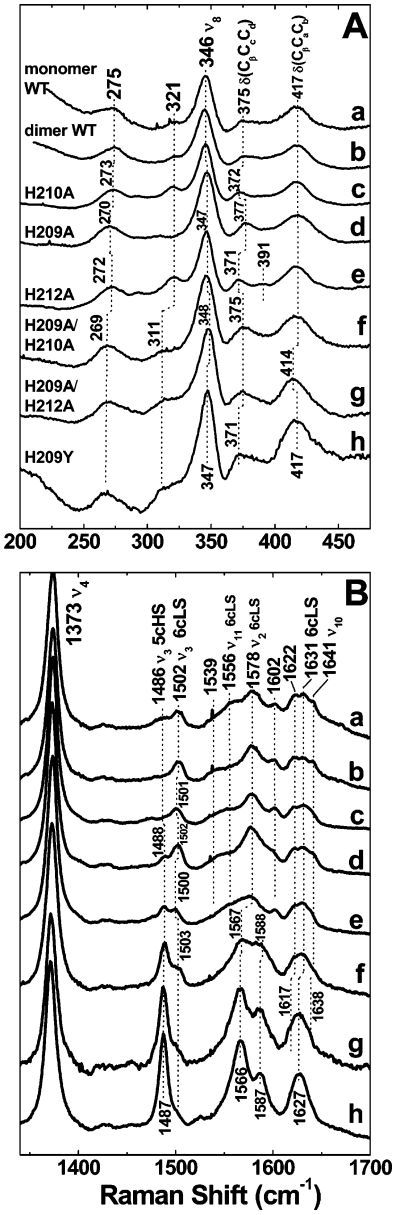

FIGURE 3: Soret-excited resonance Raman spectra of ferric PhuS and His mutants in the low-frequency (A) and in-plane porphyrin stretching (B) regions. Spectra were recorded in 20 mM Tris−HCl at pH 8.0 and correspond to (a) monomeric PhuS(WT), (b) dimeric WT, (c) H210A (58%), (d) H209A (28%), (e) H212A (98%), (f) H209A/H210A (73%), (g) H209A/H212A (90%), and (h) H209Y (97%). Numbers in parentheses indicate percentage monomer.

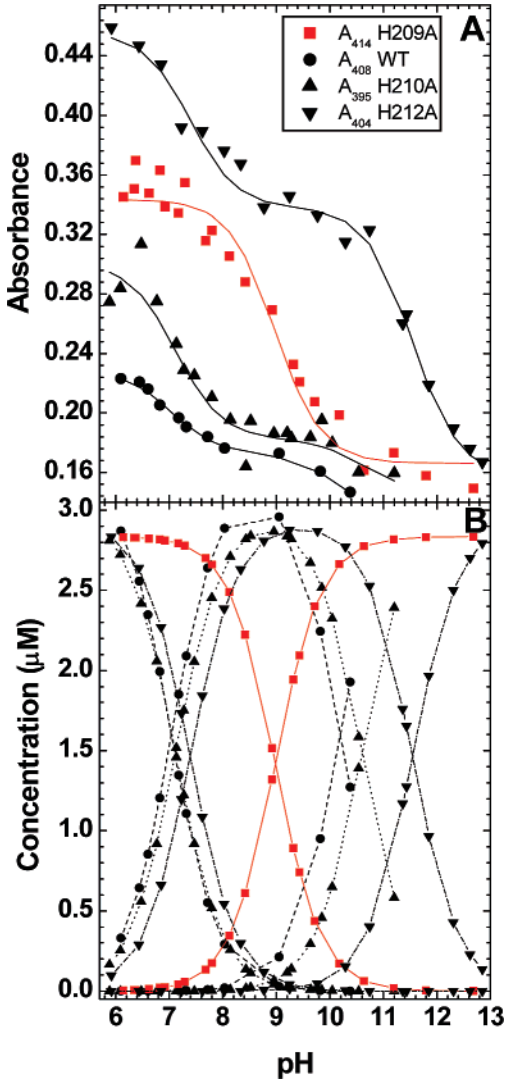

FIGURE 4: Spectrophotometric titration curves based on (A) Soret absorbance and (B) pH speciation diagrams for PhuS(WT) (58%), H209A (28%), H210A (58%), and H212A (98%). The traces for PhuS(H209A) are shown in red to punctuate its unique acid−base behavior among these constructs. Numbers in parentheses indicate percentage monomer.

In order to dissect the roles of His209 and His212 in the binding of heme, several mutations directed at these sites were constructed. The PhuS(H212A) mutant contains His210, which plays no direct role in the heme coordination chemistry of holo-PhuS (vide supra), and the conserved His209. It constitutes category III of these PhuS constructs, whose rR spectrum is dominated by 5cHS heme bands at all but the most alkaline pH (11.5). This pH trend is consistent with the presence of His-bound HS heme in acidic solution with water coordinating to a fraction of the sites. The aqua ligand is deprotonated at high pH to yield a 6cLS hydroxide complex. Histidine coordination is corroborated by a Fe−His band in the rR spectrum of ferrous PhuS(H212A) (vide infra). These rR spectra strongly support the conclusion that the ImH side chain of His209 coordinates to the heme over the pH range investigated here.

Two complementary mutations to PhuS(H212A), PhuS-(H209A) and (H209A/H210A), were also constructed. Both have histidine in position 212. As seen in Figure 5IV, and consistent with the titration curves and speciation diagrams in Figure 4, the pH dependence of the rR features for these mutants is distinct. In contrast to the other proteins reported here, the hemes in both are largely 6c and LS at low pH with conversion to 5cHS heme in alkaline solution. As such, they constitute category IV of axial ligation behavior. Although Figure 5I shows that His210 probably does not interact directly with the heme iron, it clearly influences the heme environment. For example, the scant heme loading of PhuS(H209A/H210A) (Figure 2h) indicates that the stability of the heme−PhuS(H209A/H210A) complex is lower than its H209A counterpart. Moreover, its absence influences the pK_a as 5cHS heme appears at lower pH in PhuS(H209A/H210A) than in PhuS(H209A). On the basis of the rR spectra, pK_a for the double mutant is estimated at ~5.5. Finally, 5c HS heme is more predominant at high pH in the

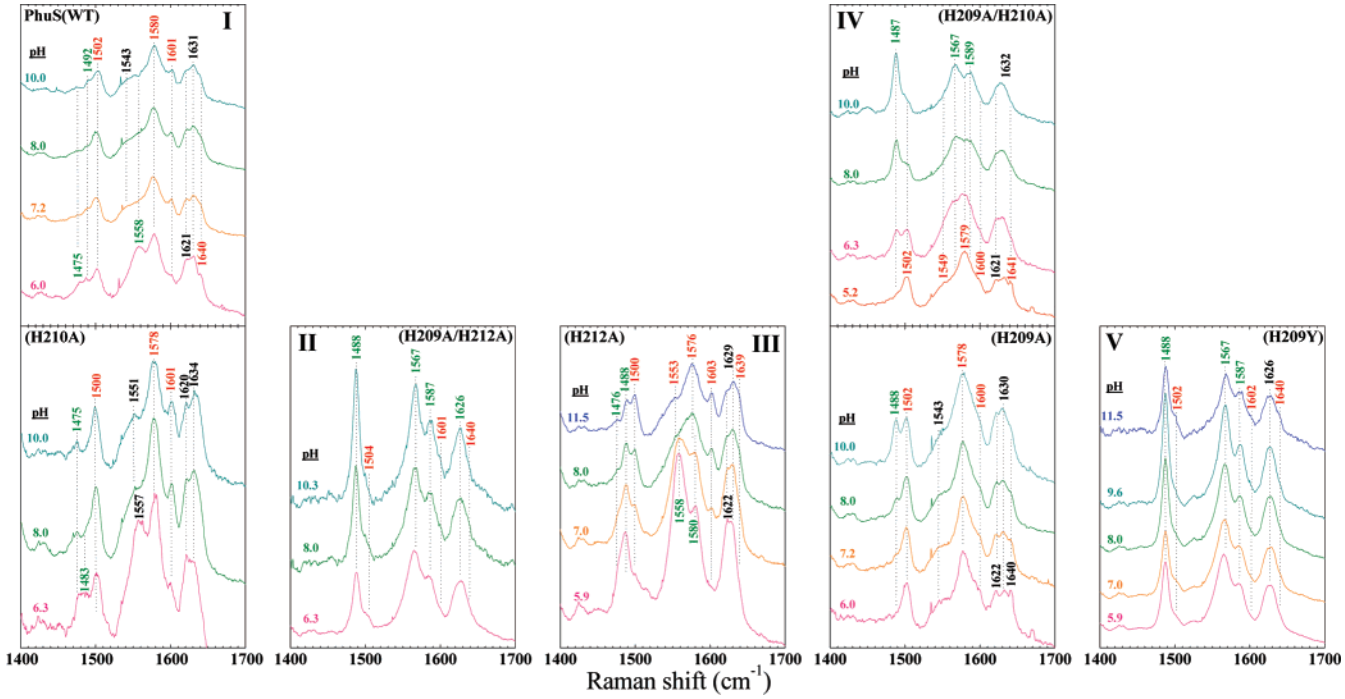

FIGURE 5: Soret-excited resonance Raman spectra of the PhuS constructs investigated in this study. Spectra were recorded under the conditions described in the Experimental Procedures. Spectra are color-coded by pH to facilitate ease of comparison between panels. Red and green frequency labels indicate bands from low-spin and high-spin hemes, respectively. Protein samples have the oligomeric composition listed in Figure 2, except WT (58%).

Table 2: Axial Ligand Environments of the Monomeric PhuS Proteins Investigated in This Study

category	PhuS mutants	available protein ligands	predominant low-pH heme states (axial ligands)	predominant high-pH heme states (axial ligands)
I	WT and H210A	His209, His212/X	6cLS (His, X) 6cHS (His, OH_2) 5cHS (His)	6cLS (His, X) (His, OH−) 6cHS (His, OH−) 5cHS (His)
II	H209A/H212A	none	5cHS (OH_2)	5cHS (OH−)
III	H212A	His209 only	6cHS (His, OH_2) 5cHS (His)	6cLS (His, OH−) 6cHS (His, OH−) 5cHS (His)
IV	H209A and H209A/H210A	His212/X	6cLS (His, X)	6cLS (His, X) 5cHS (His)
V	H209Y	His212/X Tyr209	6cLS (His, X) 5cHS (Tyr−)	6cLS (His, X) 5cHS (Tyr−)

double mutant (Figure 5IV), suggesting that His210 serves to stabilize the LS form of the His212-bound heme. This behavior suggests that in acidic solution, the heme is bound by two endogenous ligands, one of which is His212. These spectra suggest that PhuS provides an alternate axial ligand environment within the predicted binding site. Taken together with the pH dependencies described above, the protein can independently but simultaneously present the ImH side chains from His209 or His212 for coordination to the heme. The His209 complex is 5c and HS unless the pH is high enough to force OH− binding to form a 6c complex that exists as an equilibrium mixture of HS and LS heme hydroxides (*5*). By contrast, the His212 counterpart is 6c and LS, probably having two protein-based ligands. One of these ligands dissociates at high pH. Even though His212 is not conserved among the PhuS homologs, its requirement for significant LS heme population leads to the hypothesis that this second set of axial heme ligands is functionally relevant and that His212 is crucial to the stability of heme in that site.

The ability of PhuS(H209A/H212A) (category II) to retain heme with no endogenous axial ligands suggested that any properly disposed endogenous axial ligand could coordinate to the heme. To test this notion, the PhuS(H209Y) mutant was constructed. The core-size marker bands for this mutant (Figure 5V) show that it contains nearly exclusively 5cHS heme. Moreover, the υ_3/υ_4 intensity ratio (υ_4 not shown) is consistent with an anionic O-bound ligand, such as the phenolate side chain of tyrosine (*22*), over the investigated pH range. This heme is associated with the PhuS(H209Y) protein, which constitutes category V of mutants in this study. The negligible intensity attributable to LS heme bands in the rR spectra of this mutant suggests that HS heme is predominant. The lack of LS heme could be rationalized in terms of new heme coordination that requires Tyr209 *and* His212 in such a way that the coordination of Tyr209 is stabilized via H-bond acceptance by the ImH side chain of His212. Similar stabilization of Tyr coordination has been shown for ferric *Sm*HasA (*3*). Similarity between the rR

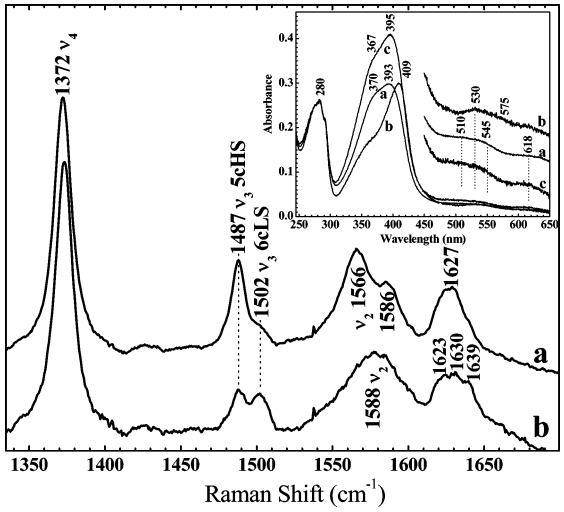

FIGURE 6: UV−vis absorbance (inset) and Soret-excited resonance Raman spectra of ferric (a) monomeric, (b) dimeric, and (c) mixed PhuS(H209A/H212A). The spectra show that 6cLS heme is favored in the dimer, even when the ligands that normally bind heme in the monomer are not present. This behavior is consistent with the presence of a heme-binding site that is assembled by dimerization.

spectra of PhuS(H209Y) and PhuS(H209/H212A) (category II, Figure 5II) raises the question of whether Tyr coordinates at all in H209Y. Attempts to observe resonance-enhanced internal Tyr modes with blue and green excitation were scuttled by photochemistry that changes the heme environment during the rR experiment. However, the fact that PhuS(H209Y) is sensitive to green light but not violet is consistent with a reactive charge transfer state that is accessible with green light in this mutant. We suggest that this is the Tyr → Fe ligand-to-metal charge-transfer (LMCT) transition. Furthermore, the contrasting UV−vis spectra in Figure 2, curves f and g, suggest that the axial ligand environments in these mutants are different.

Despite the existence of two axial heme environments, the heme/PhuS stoichiometry is 1:1 in monomeric holo-PhuS(WT). Assuming that every PhuS molecule is heme loaded, the two axial ligands interact in such a way that a single PhuS molecule can bind heme through His209 or His212, but not both.

Heme Environment in Ferrous PhuS

Resonance Raman Spectra of Ferrous PhuS(WT) and His Mutants. Ferrous PhuS(WT) and all of the aforementioned mutants were investigated using rR spectroscopy and UV−vis absorbance. The middle section of Table 1 lists the wavelengths of maximum absorbance for ferrous PhuS(WT) and the histidine mutants. The stabilities of PhuS(WT) and the His mutants are diminished in the presence of reducing agent, probably due to slow oxidative degradation by traces of peroxide, according to the previously reported mechanism (*5*). In order to slow the degradation reaction(s), spectra of the ferrous proteins were recorded at 0 °C. Figure 7C shows the high-frequency region of the 413.1 nm excited rR spectrum. The υ_4 band centered at 1359 cm^{-1} (not shown) is typical of ferrous heme. Upon reduction, υ_3 bands at 1491 and 1469 cm^{-1} indicate a mixture of 6cLS and 5cHS hemes, respectively. The visible spectrum of ferrous PhuS(WT) has been shown to contain both species, consistent with the rR data (*5*). The ferrous samples were further investigated at

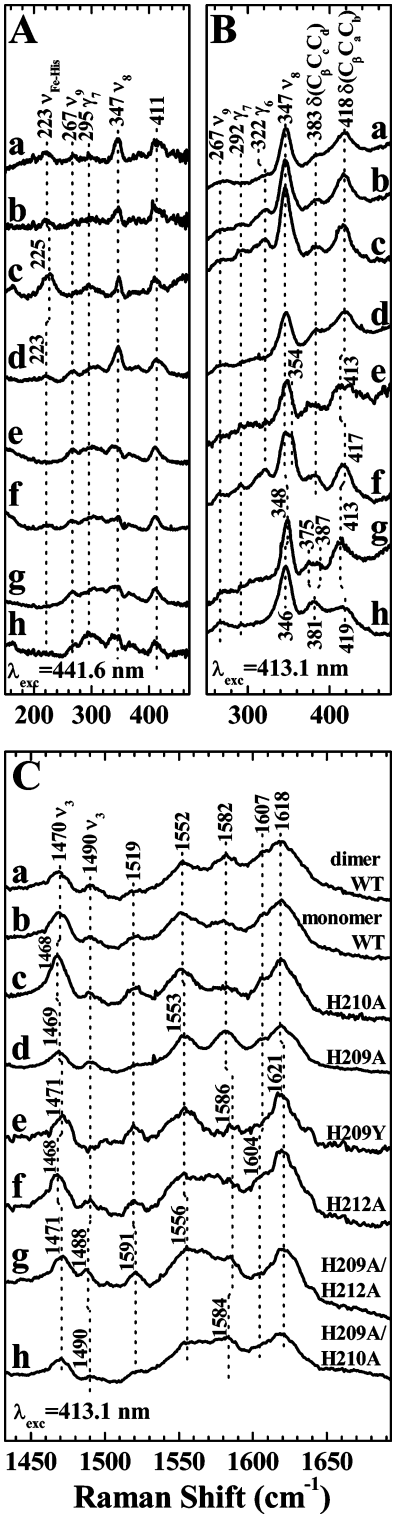

FIGURE 7: Resonance Raman spectra of the ferrous PhuS constructs using (A) 441.6 and (B and C) 413.1 nm excitation. Spectra correspond to (a) dimeric PhuS(WT), (b) monomeric WT, (c) H210A (58%), (d) H209A (28%), (e) H209Y (97%), (f) H212A (98%), (g) H209A/H212A (90%), and (h) H209A/H210A (73%). Numbers in parentheses indicate percentage monomer.

37, 20, and −20 °C. The spin state populations are temperature dependent with 6cLS heme being favored at −20 °C (data not shown). Because the ferrous proteins have short solution lifetimes, it is not clear at this time whether the temperature dependence of spin state populations reflects equilibrium populations of hemes with different axial ligand

Table 3: Low-Frequency Band Assignments for Ferrous PhuS (WT) and Histidine Mutants

ferrous heme protein	υ_{Fe-His} (cm^{-1})	υ_9 (cm^{-1})	γ_7 (cm^{-1})	γ_6 (cm^{-1})	υ_8 (cm^{-1})	$\delta_{C\beta CcCd}$ (cm^{-1})	$\delta_{C\beta CaCb}$ (cm^{-1})
WT	223	266	291	321, 312 (sh)	345	383	416
H210A	227	270	294	321, 309 (sh)	346	384	416
H212A	223[a]	266	292	321	347, 353	382	417
H209A	221[a]	269	289 (sh)[a]	306[a]	347, 332 (sh)	384	419
H209A/H210A	n/o[b]	269	300[a]	341[a]	347	381	417
H209Y	n/o[b]	267[a]	305 (sh)	335 (sh)[a]	347	380	413, 424
H209A/H212A	n/o[b]	267	n/o[b]	n/o[b]	348	375, 387	413, 423 (sh)
Mb[c]	220	240	302		342	370	405, 436
Cyt. *c*[d]		271		309 (ν_{51})		372, 382	413, 421

[a] Only detected using 441.6-nm excitation. [b] n/o, not observed. [c] Ref *23*. [d] Ref *35*.

sets or a spin state equilibrium. The low-frequency spectrum of each protein is shown for 413.1 (Figure 7B) and 441.6 nm (Figure 7A) Raman excitation. Resonance enhancement of a υ_{Fe-His} band between 200 and 245 cm^{-1} in 5c HS ferrous hemes using 441.6 nm excitation is commonly used to confirm the presence of histidine as the fifth ligand (*23*). The υ_{Fe-His} band is seen in Figure 7, parts A and B, and shown to be resonance enhanced at 223 cm^{-1} for monomeric and dimeric PhuS(WT) and at 225 cm^{-1} for PhuS(H210A) (Figure 7, parts Ac and Bc). This result is in accord with previous results for ferrous PhuS(WT) where the υ_{Fe-His} was reported at 223 cm^{-1} (*5*). PhuS(H209A) and (H212A) have υ_{Fe-His} bands, indicating that either His may coordinate to the iron center. The remaining PhuS histidine mutants (H209Y), (H209A/H210A), and (H209A/H212A) do not show resonance enhancement of a band attributable to υ_{Fe-His}. Consistent with the ferric protein, this suggests that when both His209 and His212 are replaced with noncoordinating amino acids, no other histidines coordinate to form 5c HS ferrous heme. Also, although His210 is not an axial ligand (vide supra), its mutation in (H209A/H210A) influences the stability of the His212 complex. This is manifested in a lowered pK_a when His210 is replaced by Ala in category IV (Figure 5IV). Finally, the lack of a rR band attributable to υ_{Fe-His} in the spectrum of PhuS(H209Y) is evidence that His209 is an axial ligand to HS ferrous heme PhuS(WT).

In addition to bands from Fe−L_{axial} stretching modes, the low-frequency rR spectra exhibit bands whose frequencies are sensitive to heme core and peripheral substituent conformation. Table 3 lists selected band assignments in the low-frequency range along with their observed frequencies. These bands are readily apparent in Figure 7, parts A and B. The bands near 380 and 420 cm^{-1} correspond to propionate and vinyl bending modes, respectively. Interestingly, the frequencies and widths of these bands are rather insensitive to the axial ligand environments, except for PhuS(H209A/H212A), for which the propionate bending band is split (375 and 387 cm^{-1}). Additionally, neither the frequencies nor intensities of the bands corresponding to porphyrin out-of-plane modes, γ_6 and γ_7 (Table 3), exhibit significant differences among the PhuS proteins investigated here. These insensitivities reflect porphyrin and peripheral substituent conformations that are characteristic of heme-loaded PhuS, regardless of the identities of the heme axial ligands. Thus, the nonbonded interactions between heme and protein are suggested to play a defining role in the structure of heme in the protein.

Resonance Raman Spectra of Carbonyl Complexes of PhuS(WT) and His Mutants. Resonance Raman spectroscopy provides a convenient means of determining the υ_{Fe-CO}, δ_{FeCO}, and υ_{C-O} frequencies of the FeCO moiety in heme carbonyl complexes, including PhuS−CO. The υ_{Fe-CO} and υ_{C-O} frequencies vary inversely and systematically due to the influence of electrostatic field, the associated polar interactions of the bound CO, and the donor strength of the trans ligand on the extent of FeCO π back-bonding. This well-established inverse correlation between υ_{Fe-CO} and υ_{C-O} frequencies is a basis for assessing the degree of hydrogen bonding (most evident in υ_{C-O}) and the donor strength (i.e., identity) of the proximal ligand. Frequencies of the aforementioned FeCO modes were determined and confirmed using ^{13}CO isotope editing for PhuS(WT) and the histidine mutants. Figure 8A shows the rR spectrum of each protein in the fingerprint region wherein υ_4, the π^* electron density marker, at 1371 cm^{-1} (not shown) is characteristic of ferrous heme coordinated to a π-acceptor ligand and υ_3, the spin state marker, at 1496 cm^{-1} is typical of 6cLS ferrous heme. The CO stretching region of the spectrum (Figure 8B) exhibits a band near 1960 cm^{-1}, which is assigned to υ_{C-O} based on ^{13}CO isotope shifts for PhuS(WT) and the previously mentioned histidine mutants. The 1951 cm^{-1} band is assigned to the υ_{C-O} mode of aqueous heme−CO. The difference spectra showing the ^{13}CO isotope shift is shown in Figure 8C. The low-frequency parent and difference spectra are shown in Figure 9, parts A and B, for the natural abundance and ^{13}CO complexes of PhuS(WT) and mutants. The spectra in Figure 9 fall into two groups, those exhibiting one υ_{Fe-CO} band and those with two. The low-frequency spectra of PhuS(WT) (Figure 9Aa) and (H210A) (Figure 9Ab) have a similar appearance and contain one υ_{Fe-CO} band. PhuS(H209A) (Figure 9Ac) similarly displays one sharpened υ_{Fe-CO} band but shows slight differences in the lower-frequency band shapes and intensities where differences in porphyrin conformation are manifested (*23*, *24*). In particular, υ_8 is shifted 6 cm^{-1} to lower frequency, suggesting an altered heme environment in (H209A) compared to (WT) and (H210A). The sharpening of the υ_{Fe-CO} band and shift in υ_8 in the spectrum of (H209A) are consistent with loss of the His209 binding site (vide supra).

All of the other PhuS−CO spectra in Figure 9d−g exhibit *two* υ_{Fe-CO} bands. The higher frequency band occurs at a position similar to that of free heme−CO at neutral pH, suggesting that it is 5c or has a weak-field ligand bound trans to CO (vide infra). The species giving rise to these bands will hereinafter be referred to as 5c heme−CO complexes. Interestingly, the 5c CO complexes only appear in the PhuS mutants where the putative His212 binding site is either directly or indirectly disrupted. Direct disruption is affected

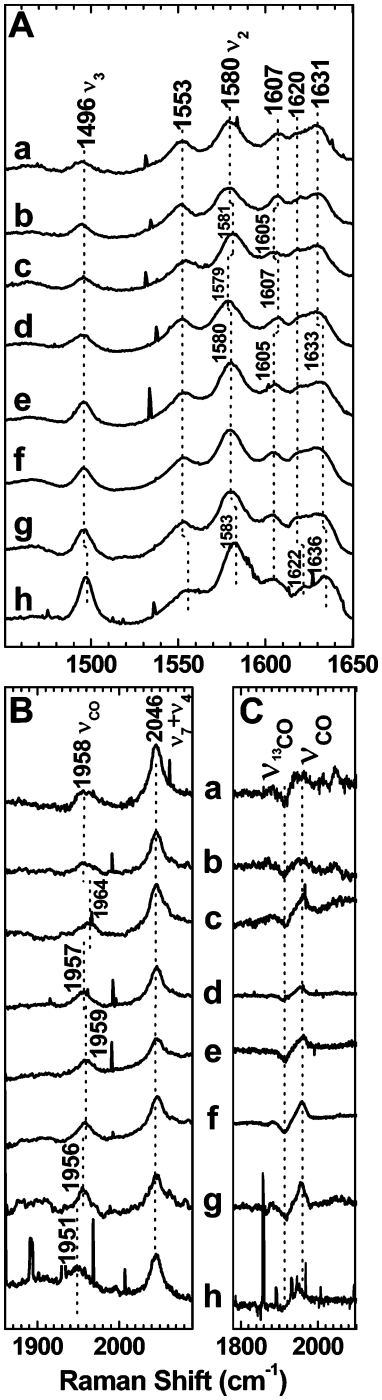

FIGURE 8: Soret-excited resonance Raman spectra of PhuS−CO complexes investigated in this study in the (A) porphyrin in-plane stretching and (B and C) C−O stretching ranges. Spectra correspond to (a) PhuS(WT) (58%), (b) H210A (58%), (c) H209A (28%), (d) H212A (98%), (e) H209/H210A (73%), (f) H209Y (97%), (g) H209A/H212A (90%), and (h) aqueous heme−CO. Numbers in parentheses indicate percentage monomer.

by replacing His212 with a noncoordinating amino acid, as in (H212A) and (H209A/H212A). Indirect disruption results from either replacing His210 with a noncoordinating amino acid or from replacing His209 with tyrosine, whose coordinating phenol side chain interacts with His212 (vide supra). The λ_{max} for visible absorbance of the CO complexes are listed in the bottom section of Table 1. The presence of a 5c heme−CO species is evident in the blue-shifted Soret absorbances of the mutant complexes. This is especially true

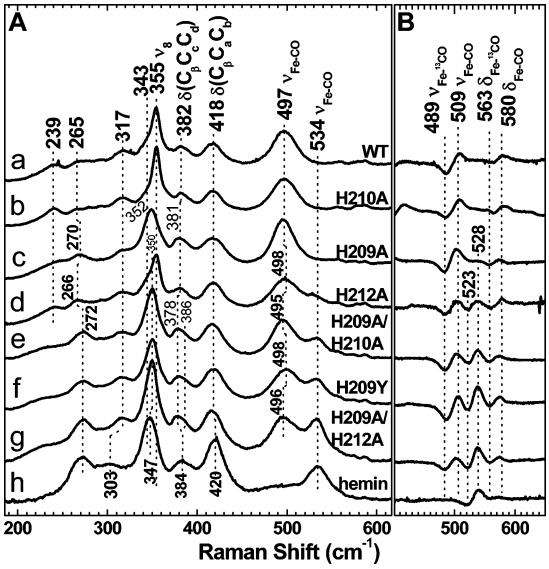

FIGURE 9: Resonance Raman spectra of PhuS−CO complexes in (A) the Fe−CO stretching region and (B) the corresponding ^{13}C isotope difference spectra. Traces correspond to (a) PhuS(WT) (58%), (b) H210A (58%), (c) H209A (28%), (d) H212 A (98%), (e) H209A/H210A (73%), (f) H209Y (97%), (g) H209A/212A (90%), and (h) aqueous heme−CO. Numbers in parentheses indicate percentage of monomer.

of (H209A/H212A) whose λ_{max} closely matches that of free heme−CO and of the HO mutants HmuO(H20A)−CO from *Corynebacterium diphtheriae* (*25*) and HO-1(H25A) (*26*). This is in accord with the low-frequency rR spectrum of (H209A/H212A), which exhibits the largest 5c υ_{Fe-CO} rR band of all the mutants. Interestingly, even when both His209 and His212 are replaced, a species whose frequencies are consistent with a proximal (trans) histidine ligand persists (Figure 9Ag). This suggests that another His residue, possibly the nearby His210, substitutes for the mutated histidines.

The placement of the υ_{Fe-CO} and υ_{C-O} frequencies onto the back-bonding correlation plot in Figure 10 shows that PhuS(WT), (H209A), and (H210A) fall in a tight cluster low on the proximal histidine line. These frequencies are typical of 6c CO complexes with the imidazole side chain of histidine as the trans ligand (*27*). PhuS(H212A), (H209A/H210A), (H209Y), and (H209A/H212A), all of which exhibit multiple heme−CO species, comprise one component that is similar to (WT) and a second component that lies above the histidine line in a region typically associated with 5c CO complexes or complexes whose sixth ligand is weak, such as tyrosinate or water (*27*). This assignment as 5c or 6c with trans-OH_2 is based on comparison of the PhuS heme carbonyls with the complex obtained from reaction of aqueous hemin chloride with dithionite and CO (Figure 9Ah).

Heme Environment in Dimeric PhuS

Apo-PhuS(WT) and the mutants investigated in this study are isolated as mixtures of monomer, dimer, and trimer (*5*). Once established, the dimer population is unaffected by varying salt concentration, pH buffering system, or pH. Purified dimer, whether heme loaded or not, does not dissociate to monomer to any measurable extent on the time scale of weeks. Because its stability does not require bound heme, it seems likely that the dimer contains significant intermolecular surface contacts.

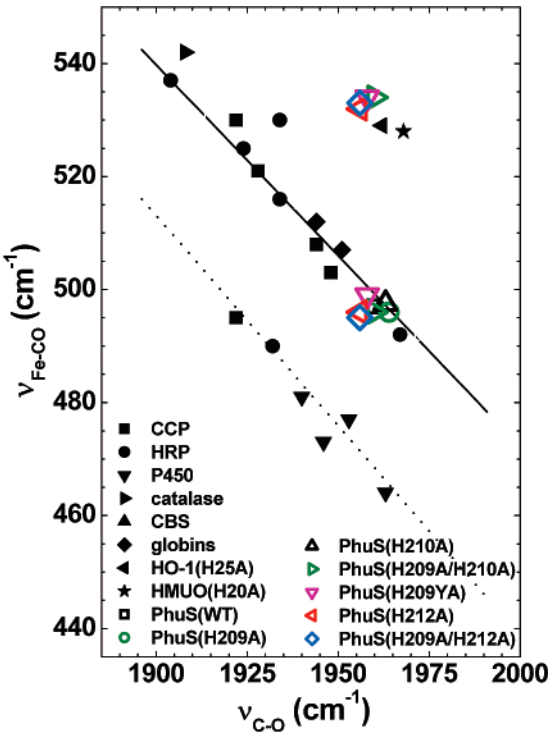

FIGURE 10: FeCO back-bonding correlation plot showing selected heme carbonyls in the six-coordinate category with anionic (dotted line) and neutral ImH (solid line) ligands trans to CO and in the five-coordinate category (top cluster, no line). PhuS points are color-coded according to the corresponding categories of ferric PhuS constructs discussed in the text. PhuS samples have the composition given for Figure 9.

PhuS(H209A/H212A), whose monomer provides no endogenous ligands in its monomeric heme-binding pocket (vide supra), contains a significant amount of 6cLS heme. In fact, all dimers which could be isolated in quantities large enough to record UV−vis and rR spectra (WT (Figures 2b and 3b), H209A, H209A/H210A, and H209A/H212A (Figure 6)) exhibit 6c LS heme signatures. These observations suggest that there is a second heme-binding site that is assembled upon dimerization of PhuS, reminiscent of the domain-swapped dimer of *Sm*HasA, which has been proposed to serve as a heme reservoir in vivo (*28*). In the case of PhuS, the heme would bridge the dimer by coordinating two ligands, one from each of two PhuS molecules. Although PhuS, ShuS, HemS, and ChuS are structurally distinct from *Sm*HasA and even though it is not clear whether their dimers are of the domain-swapped type, the possibility that PhuS forms a heme-binding site upon dimerization suggests that their protein−protein associations could have similar roles.

DISCUSSION

The results reported here identify two histidine residues, His209 and His212, that are involved in the binding of heme by monomeric PhuS. The histidine at position 209 is strictly conserved in the bacterial cytoplasmic heme-binding proteins, but His212 is not. Both are located in the C-terminal domain and, based on the homology model, on a helix analogous to those bearing the heme ligands in holo-HemS and holo-ChuS. These two histidine residues constitute alternate ligands in the monomeric PhuS binding site whose occupancies within a single PhuS molecule are mutually exclusive. Whether the relative populations of these sites is determined by equilibrium or kinetic considerations is currently unknown and is a topic of ongoing investigation. If the His212 ligand is physiologically relevant, then the presence of two heme ligands within the same binding site raises interesting questions as to the function of PhuS. Additionally, a binding site unique to dimeric PhuS has been observed. Although the axial heme ligands of this site remain to be identified, the ligands are not side chains from His209 or His212. The fact that this site is only populated in the dimer suggests that it comprises ligands from two protein molecules. Whether it is actually a domain-swapped structure remains to be determined. However, it seems likely that the dimer contains significant intermolecular surface contacts, as its stability does not require bound heme.

Multiple Heme-Binding Sites. PhuS is unique among the cytoplasmic heme-binding proteins characterized to date in having the alternate His212 ligand in the "crystallographic" binding site. However, sequence analysis and examination of the holo-HemS and holo-ChuS structures suggest it may not be unique in having multiple heme-binding sites. Specifically, PhuS, ShuS, HemS, and ChuS contain another conserved His residue (PhuS, His293; ShuS, His277; HemS, His280; ChuS, His277). Strict conservation of this coordinating residue raises the possibility that it could also play a role in heme binding. However, this remains to be addressed experimentally.

Role of PhuS. At present, there is considerable evidence to support a role for holo-PhuS in delivering heme to *Pa*HO (*5*, *31*). While the heme in holo-PhuS is converted to verdoheme in the presence of O_2 and a reducing agent, the reaction is scuttled if O^{2-} and H_2O_2 are scavenged by addition of catalase and superoxide dismutase (*5*). Thus PhuS does not produce verdoheme by the classical HO mechanism; its role in heme metabolism is indirect.

One possible explanation for alternate heme-binding ligands in PhuS is that they are sequentially populated during heme uptake or heme release to *Pa*HO. In this case, population of both sites in the purified protein would probably be a kinetic artifact of not loading the PhuS with its natural heme donor. This explanation is mechanistic and is not predicated on a separate function.

Another plausible role for either alternate heme-binding ligands, or the second binding site, is that they could support multiple functions of PhuS in vivo. Although any function in addition to heme trafficking is a matter of speculation at this time, there are some interesting possibilities. One example might be sensing of cytoplasmic heme availability for purposes of cellular regulation. A scavenger of cytoplasmic heme and/or a heme storage reservoir is another plausible function of PhuS. Insofar as multiple heme states in holo-PhuS intimate multiple functions, the dependencies of coordination number and spin state on pH and heme oxidation state described herein indicate that those functions may be toggled by variabilities in cytosolic pH and reduction potential. Additionally, the formation of PhuS oligomers could play a role in heme storage by forming new heme-binding sites at the protein interface, as has been shown for the domain-swapped dimers of HasA (*28*−*30*). While bacterial proteins, such as CooA (*32*), having multiple sensing functions have been extensively characterized, no proteins having multiple, reversible heme-binding functions have been reported to date.

Comparison of the sequence homologies between the Gram-negative cytoplasmic heme-binding proteins that have been physically and/or chemically characterized to date reveals interesting similarities and contrasts. In addition to their striking sequence homology, the ChuS and ShuS proteins share a tendency to form oligomers in solution (*7*, *10*). Although, the physiological relevance of oligomerization is not presently clear, it has been hypothesized to play a role in the binding of ShuS to DNA (*34*). The tendency of PhuS to form dimers and trimers in solution suggests that it too may bind to DNA, although this has yet to be established. The *chu* and *shu* operons in *E.coli* O157:H7 and *S. dysenteriae*, respectively, bear a strong similarity that is not shared with the *phu* operon from *P. aeruginosa*. Specifically, the *shuS* and *chuS* genes are transcribed downstream from the outer membrane receptor genes (*shuA* and *chuA*) (*33*). By contrast, the *phuS* gene in *P. aeruginosa* is located upstream from the outer membrane receptor and is divergently transcribed (*4*), suggesting the possibility that it is regulated differently and has different or additional function(s).

SUMMARY

The resonance Raman and mutagenesis results presented herein reveal that PhuS harbors two heme-binding sites. This combined approach has identified a site in monomeric PhuS having alternate His ligands at positions 209 (one endogenous ligand) and 212 (two endogenous ligands). A second binding site is present in dimeric PhuS and harbors 6cLS heme, even when both the His209 and His212 residues are mutated to Ala. The presence of conserved residues that are potential heme ligands in all of the homologs characterized to date suggest that the dimer could be cross-linked by bound heme.

The presence of multiple heme-binding sites suggests the possibility that these cytoplasmic heme-binding proteins have multiple functions. Among the possibilities are sensing and scavenging/storage of heme. The physiological relevance of these sites is the subject of ongoing investigation.

REFERENCES

1. Wandersman, C., and Stojiljkovic, I. (2000) Bacterial heme sources: the role of heme, hemoprotein receptors and hemophores, *Curr. Opin. Microbiol. 3*, 215−220.
2. Wandersman, C., and Delepelaire, P. (2004) Bacterial iron sources: From siderophores to hemophores, *Annu. Rev. Microbiol. 58*, 611−647.
3. Arnoux, P., Haser, R., Izadi, N., Lecroisey, A., Delepierre, M., Wandersman, C., and Czjzek, M. (1999) The crystal structure of HasA, a hemophore secreted by Serratia marcescens, *Nat. Struct. Biol. 6*, 516−520.
4. Ochsner, U. A., Johnson, Z., and Vasil, M. L. (2000) Genetics and regulation of two distinct haem-uptake systems, phu and has, in *Pseudomonas aeruginosa*, *Microbiology (Reading, U.K.) 146 (Part 1)*, 185−198.
5. Lansky, I. B., Lukat-Rodgers, G. S., Block, D., Rodgers, K. R., Ratliff, M., and Wilks, A. (2006) The cytoplasmic heme-binding protein (PhuS) from the heme uptake system of *Pseudomonas aeruginosa* is an intracellular heme-trafficking protein to the d-regioselective heme oxygenase, *J. Biol. Chem. 281*, 13652−13662.
6. Schneider, S., Sharp, K. H., Barker, P. D., and Paoli, M. (2006) An induced fit conformational change underlies the binding mechanism of the heme transport proteobacteria-protein HemS, *J. Biol. Chem. 281*, 32606−32610.
7. Suits, M. D. L., Jaffer, N., and Jia, Z. (2006) Structure of the *Escherichia coli* O157:H7 heme oxygenase ChuS in complex with heme and enzymatic inactivation by mutation of the heme coordinating residue His-193, *J. Biol. Chem. 281*, 36776−36782.
8. Suits, M. D. L., Pal, G. P., Nakatsu, K., Matte, A., Cygler, M., and Jia, Z. (2005) Identification of an *Escherichia coli* O157:H7 heme oxygenase with tandem functional repeats, *Proc. Natl. Acad. Sci. U.S.A. 102*, 16955−16960.
9. Wyckoff, E. E., Lopreato, G. F., Tipton, K. A., and Payne, S. M. (2005) *Shigella dysenteriae* ShuS promotes utilization of heme as an iron source and protects against heme toxicity, *J. Bacteriol. 187*, 5658−5664.
10. Wilks, A. (2001) The ShuS protein of *Shigella dysenteriae* is a heme-sequestering protein that also binds DNA, *Arch. Biochem. Biophys. 387*, 137−142.
11. Buchanan, S. K., Smith, B. S., Venkatramani, L., Xia, D., Esser, L., Palnitkar, M., Chakraborty, R., Van Der Helm, D., and Deisenhofer, J. (1999) Crystal structure of the outer membrane active transporter FepA from *Escherichia coli*, *Nat. Struct. Biol. 6*, 56−63.
12. Schwede, T., Kopp, J., Guex, N., and Peitsch, M. C. (2003) Swiss-Model: an automated protein homology-modeling server, *Nucleic Acids Res. 31*, 3381−3385.
13. Guex, N., and Peitsch, M. C. (1997) Swiss-Model and the Swiss-PdbViewer: An environment for comparative protein modelling, *Electrophoresis 18*, 2714−2723.
14. Peitsch, M. C. (1995) Protein modeling by E-mail, *Bio/Technology 13*, 658−660.
15. Jin, Y., Nagai, M., Nagai, Y., Nagatomo, S., and Kitagawa, T. (2004) Heme structures of five variants of hemoglobin M probed by resonance Raman spectroscopy, *Biochemistry 43*, 8517−8527.
16. Oellerich, S., Wackerbarth, H., and Hildebrandt, P. (2002) Spectroscopic characterization of nonnative conformational states of cytochrome *c*, *J. Phys. Chem. B 106*, 6566−6580.
17. Maes, E. M., Walker, F. A., Montfort, W. R., and Czernuszewicz, R. S. (2001) Resonance Raman spectroscopic study of nitrophorin 1, a nitric oxide-binding heme protein from *Rhodnius prolixus*, and its nitrosyl and cyano adducts, *J. Am. Chem. Soc. 123*, 11664−11672.
18. Wang, J., Stuehr, D. J., Ikeda-Saito, M., and Rousseau, D. L. (1993) Heme coordination and structure of the catalytic site in nitric oxide synthase, *J. Biol. Chem. 268*, 22255−22258.
19. Das, T. K., Boffi, A., Chiancone, E., and Rousseau, D. L. (1999) Hydroxide rather than histidine is coordinated to the heme in five-coordinate ferric *Scapharca inaequivalvis* hemoglobin, *J. Biol. Chem. 274*, 2916−2919.
20. Chan, A. C. K., Lelj-Garolla, B., Rosell, F. I., Pedersen, K. A., Mauk, A. G., and Murphy, M. E. P. (2006) Cofacial heme binding is linked to dimerization by a bacterial heme transport protein, *J. Mol. Biol. 362*, 1108−1119.
21. Wood, B. R., Langford, S. J., Cooke, B. M., Lim, J., Glenister, F. K., Duriska, M., Unthank, J. K., and McNaughton, D. (2004) Resonance Raman spectroscopy reveals new Insight into the electronic structure of b-hematin and malaria pigment, *J. Am. Chem. Soc. 126*, 9233−9239.
22. Eakanunkul, S., Lukat-Rodgers, G. S., Sumithran, S., Ghosh, A., Rodgers, K. R., Dawson, J. H., and Wilks, A. (2005) Characterization of the periplasmic heme-binding protein ShuT from the heme uptake system of *Shigella dysenteriae*, *Biochemistry 44*, 13179−13191.
23. Hu, S., Smith, K. M., and Spiro, T. G. (1996) Assignment of protoheme resonance Raman spectrum by heme labeling in myoglobin, *J. Am. Chem. Soc. 118*, 12638−12646.
24. Shi, Z., Franco, R., Haddad, R., Shelnutt, J. A., and Ferreira, G. C. (2006) The conserved active-site loop residues of ferrochelatase induce porphyrin conformational changes necessary for catalysis, *Biochemistry 45*, 2904−2912.
25. Wilks, A., and Moenne-Loccoz, P. (2000) Identification of the proximal ligand His-20 in heme oxygenase (Hmu O) from *Corynebacterium diphtheriae*. Oxidative cleavage of the heme macrocycle does not require the proximal histidine, *J. Biol. Chem. 275*, 11686−11692.
26. Sun, J., Loehr, T. M., Wilks, A., and Ortiz de Montellano, P. R. (1994) Identification of histidine 25 as the heme ligand in human liver heme oxygenase, *Biochemistry 33*, 13734−13740.
27. Spiro, T. G., and Wasbotten, I. H. (2005) CO as a vibrational probe of heme protein active sites, *J. Inorg. Biochem. 99*, 34−44.

28. Czjzek, M., Letoffe, S., Wandersman, C., Delepierre, M., Lecroisey, A., and Izadi-Pruneyre, N. (2007) The crystal structure of the secreted dimeric form of the hemophore HasA reveals a domain swapping with an exchanged heme ligand, *J. Mol. Biol. 365*, 1176−1186.
29. Bennett, M. J., and Eisenberg, D. (1994) Refined structure of monomeric diphtheria toxin at 2.3 .ANG. resolution, *Protein Sci. 3*, 1464−1475.
30. Yang, S., Cho, S. S., Levy, Y., Cheung, M. S., Levine, H., Wolynes, P. G., and Onuchic, J. N. (2004) Domain swapping is a consequence of minimal frustration, *Proc. Natl. Acad. Sci. U.S.A. 101*, 13786−13791.
31. Bhakta, M. N., and Wilks, A. (2006) The mechanism of heme transfer from the cytoplasmic heme binding protein PhuS to the delta-regioselective heme oxygenase of *Pseudomonas aeruginosa*, *Biochemistry 45*, 11642−11649.
32. Roberts, G. P., Kerby, R. L., Youn, H., and Conrad, M. (2005) CooA, a paradigm for gas sensing regulatory proteins, *J. Inorg. Biochem. 99*, 280−292.
33. Wyckoff, E. E., Duncan, D., Torres, A. G., Mills, M., Maase, K., and Payne, S. M. (1998) Structure of the *Shigella dysenteriae* heme transport locus and its phylogenetic distribution in enteric bacteria, *Mol. Microbiol. 28*, 1139−1152.
34. Kaur, A. P., and Wilks, A. (2007) Heme inhibits the DNA binding properties of the cytoplasmic heme binding protein of *Shigella dysenteriae* (ShuS), *Biochemistry 46*, 2994−3000.
35. Hu, S., Morris, I. K., Singh, J. P., Smith, K. M., and Spiro, T. G. (1993) Complete assignment of cytochrome *c* resonance Raman spectra via enzymic reconstitution with isotopically labeled hemes, *J. Am. Chem. Soc. 115*, 12446−12458.

BI701509N